Structural properties of chlorinated epitaxial C_{60} films

S. Woedtke, A. Meeder, R. Adelung, R. Schwedhelm, L. Kipp,* and M. Skibowski
Institut für Experimentelle und Angewandte Physik, Universität Kiel, D–24118 Kiel, Germany
(Received 9 May 2000; published 22 March 2001)

The interaction of chlorine gas with epitaxially grown C_{60} films was investigated by combined scanning tunneling microscopy (STM) x-ray photoelectron spectroscopy (XPS) and x-ray absorption spectroscopy (XANES). The STM measurements of chlorinated fullerene surfaces on VSe_2 reveal an inhomogeneous C_{60} and chlorine coverage in an area up to 200 nm from the fullerene island edges but showed no influence to the fullerene (111) coordination in the inner regions of the layers. In accordance with the STM data the XPS spectra of C 1*s* and Cl 2*p* core levels, which were taken at different emission angles, provide evidence for chlorine aggregation on the fullerite surface. As valence band and XANES spectra show that all C_{60} features derived from the highest occupied and lowest unoccupied molecular orbitals are preserved, a noncovalent interaction between fullerene and halogen can be concluded. As monitored by STM subsequent fullerene deposition on the chlorinated samples prove the perturbed island areas to serve as growth seeds so that a chlorine incorporation into the fullerite lattice can be achieved by an alternating preparation sequence.

DOI: 10.1103/PhysRevB.63.155401 PACS number(s): 68.55.Ln, 71.20.Tx, 79.60.−i

I. INTRODUCTION

Since the discovery of C_{60} (Ref. 1) as a new form of carbon and since the breakthrough in the synthesis of macroscopic quantities,[2] the physical and electronic properties of C_{60} have been widely studied. A significant characteristic of C_{60} single crystals is the possibility of *n*-type doping by the use of alkali metals, which may lead to superconducting fulleride phases[3–5] with transition temperatures up to 40 K.[6] Thereby charge transfer from alkali-metal atoms located at the tetrahedral and octahedral sites of the C_{60} fcc lattice to the threefold degenerate lowest unoccupied molecular orbital[7] (LUMO) band of the fullerene leads to the formation of a strongly bonded ionic metal.[8] In contrast, acceptor doping in solid C_{60} has not been reported so far, although the depletion of the fivefold degenerate highest occupied molecular orbital[7] (HOMO) promises to lead to superconductors with generally higher transition temperatures.[9] A major problem for hole injection into C_{60} lies in its chemical behavior comparable to large atoms of group VI or VII from the periodic table of the elements.[10] So only halogens exhibit suitable electron affinities to serve as electron acceptors for C_{60}. The understanding of the halogen-fullerene interaction is therefore of general interest.

A number of experimental studies on this subject has been published, establishing two kinds of halogen-fullerene compounds. First, reactions of C_{60} powder or solution with elemental halogens (vapor pressure in the range of several atmospheres) have been reported, forming covalently bonded $C_{60}X_n$ (X=Br,Cl,F) (Refs. 11–15) for a wide variety of *n* values. However, these products show neither physical nor chemical similarities to the alkali-metal–fullerene compounds.[16] On the other hand, in the case of iodine stoichiometries with significantly lower halogen concentrations have been found. Raman scattering[16,17] and x-ray diffraction studies[18,19] of $C_{60}I_{4-x}$ confirmed the intercalation of iodine molecules into the fullerite lattice forming a van der Waals–type bonding with the C_{60} molecules. Unfortunately only in a few studies halogenation carried out on epitaxially grown C_{60} films under UHV conditions so that photoelectron spectroscopy could be applied to the iodine-incorporated samples. Werner and co-workers[20] found a valence band structure completely different from pristine fullerite while Ohno and co-workers[21] observed C 1*s* core level shifts that were analogous but in the opposite direction to those observed in K_xC_{60} layers. However, information about the chemical interaction or the location of the iodine particles relative to the C_{60} film surface was not provided. Furthermore, the influence of other halogens than iodine was not examined, although chlorine or flourine exhibit more suitable attributes for charge transfer or intercalation effects comparable to the alkali-metal atoms. Therefore the structural properties of halogenated fullerite surfaces remain uncertain so far.

It is the aim of the present paper to investigate the interaction of chlorine gas with fullerene samples grown by molecular beam epitaxy (MBE). In order to distinguish between covalent and noncovalent bonding and to study an eventual interdiffusion of the halogen particles, chlorinated fullerene films were studied via scanning tunneling microscopy (STM) revealing a noticeable halogen-induced perturbance to the (111) coordination of the C_{60} molecules. The STM results are then discussed in comparison with photoelectron spectra that provide surface-sensitive information about the electronic structure of the samples. In view of possible analogies to alkali-metal doping, special effort is made to prove that the cage structure of C_{60} is conserved and will not be affected by the halogen, as was taken into account by Miyamoto and co-workers.[22] Additional x-ray photoelectron spectroscopy (XPS) measurements of the C 1*s* and Cl 2*p* core levels that were performed under different emission angles and probed the chlorine concentration at different information depths give evidence for a halogen aggregation on the fullerite surface so that the structural changes can be attributed to the adsorption of chorine particles. Finally, we conclude by presenting a preparation method with an alternating chlorine and fullerene deposition sequence. As shown with the help of STM measurements a multilayered structure is

formed that allows the incorporation of halogen particles into the C_{60} lattice.

II. SAMPLE PREPARATION AND EXPERIMENTAL SETUP

A previous STM study[23] was used to point out that the use of layered VSe_2 substrates allows the epitaxial accommodation of C_{60} molecules because of rather small van der Waals forces at the surface and because of a suitable lattice parameter. Due to its two-dimensional structure the material can be easily cleaved *in vacuo*, producing well-ordered surfaces with a low density of defects. All results described in this paper were obtained from $C_{60}(111)$ films grown on VSe_2 via MBE. C_{60} molecules[24] were evaporated from a temperature-controlled effusion cell at 565 K. Using a resistive heating unit mounted on the sample holder, the substrate temperatures were tunable from room temperature up to 550 K. During the fullerene evaporation the total pressure in the epitaxy chamber was in the lower 10^{-10} mbar range monitored by a mass spectrometer. The thickness of the deposited material was estimated by STM so that temperature-dependent parameters for single-monolayer deposition could be derived. After C_{60} evaporation, chlorine gas[25] was led into the preparation chamber using a leak valve. The chlorine partial pressure determined from the characteristic peaks in the mass spectrum was then adjusted to a maximum value of 6×10^{-6} mbar. After the chlorination, which never exceeded 60 min the leak valve was closed so that the total pressure could be decreased again. After UHV conditions had been established again the samples were transferred into the STM chamber without breaking the vacuum.

The STM used for the topographic measurements consists[26] of a single-tube scanner mounted on a vibration damping with an eddy current attenuation. The tips were produced by etching tungsten wire and are changeable by transfer in the UHV system. For calibration, length scales of silicon crystals were used. Positive bias voltage corresponds to electrons tunneling into empty states of the sample. All STM images were taken at room temperature in the constant current mode, where I_T denotes the tunneling current.

Using a transportable vacuum chamber the samples were then transferred to the undulator beamline BW3 of the positron storage ring DORIS III at the Hamburg Synchrotron Radiation Laboratory (HASYLAB), where the photoemission measurements were carried out. Photon energies were adjustable from 40 eV to 1500 eV. For photon energy calibration of the SX 700 monochromator, the binding energies of suitable core levels were determined to first and second order, resulting in a remaining energy uncertainty of about 20 meV. The photoelectrons were detected by a 180° spherical analyzer mounted on a two axis goniometer with an angular precision better than 0.2°. The binding energies in the ultraviolet photoelectron spectroscopy (UPS) and XPS spectra were referenced to the Fermi level, which was determined independently from a polycrystalline gold sample on a similar sample holder with an accuracy of 10 meV. An energy resolution of 125 meV was chosen for the photoemission and for the x-ray absorption spectroscopy (XANES) measurements. XANES investigations were performed in the constant final energy mode of photoemission for low kinetic energies (3.5 eV).

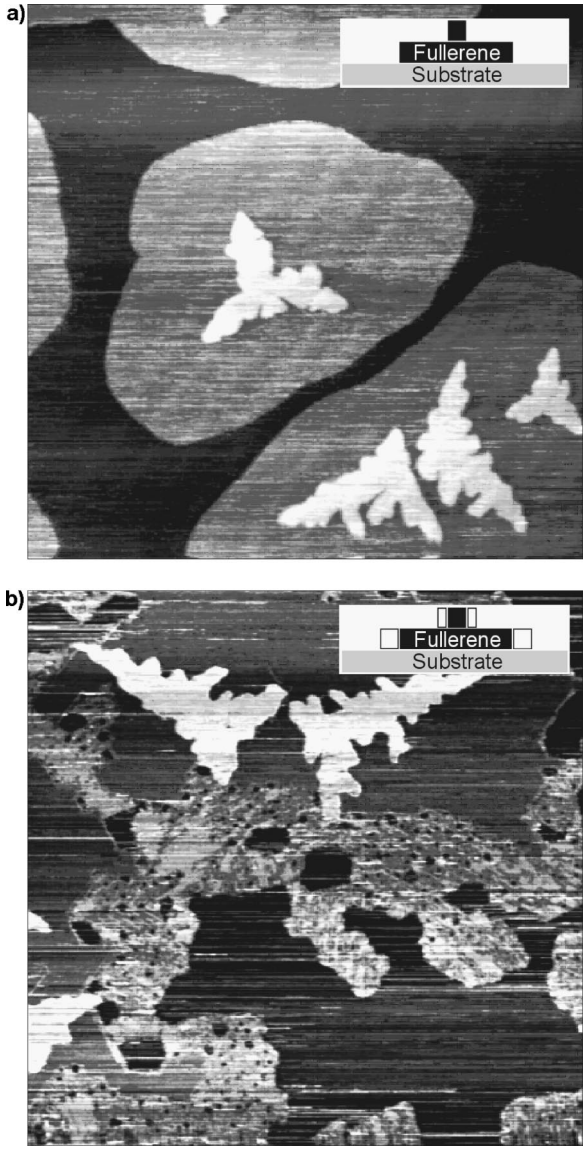

FIG. 1. STM images of 0.64 monolayer C_{60} on VSe_2 before (a) and after (b) exposure to 13 500 langmuir (1 langmuir = 1 L $= 10^{-6}$ Torr sec chlorine gas. The halogen influence is discernible at the island edges but not in the inner cluster regions (dimension, 1000×1000 nm^2; bias, +1.52 V; $I_T = 0.57$ nA).

III. RESULTS AND DISCUSSION

Figure 1 depicts a series of STM images illustrating the fullerene sample morphology before and after chlorination. At first an amount of 0.64 monolayers C_{60} was deposited onto a VSe_2 substrate heated to 340 K. In accordance to former results[23] this leads to the formation of roundish islands in the first monolayer (about 400 nm diameter) capped with tiny fractal-like clusters of the second layer (up to 200 nm diameter), which is shown in a 1000×1000 nm^2 area in Fig. 1(a). A schematic diagram in the top right corner under-

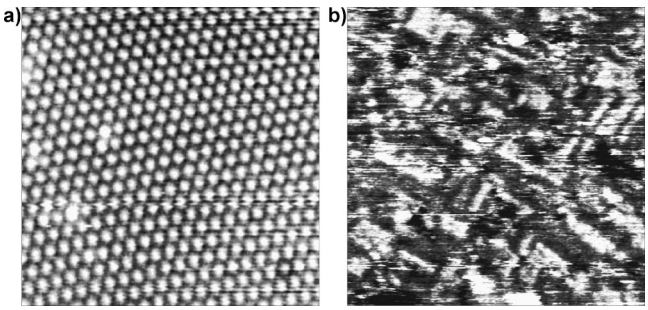

FIG. 2. STM images of the inner (a) and the outer (b) fullerene island edges of Fig. 1(b). Due to chlorine aggregation in the edge regions the coverage has become inhomogeneous. No single C_{60} molecules are identifiable (dimension, (a) 17×17 nm^2; (b) 60×60 nm^2, bias, $+1.5$ V, $I_T=0.57$ nA).

scores this fact with a side view. It is noteworthy to state that additional STM measurements confirmed a perfectly hexagonal arrangement of the molecules, indicating an epitaxial (111) growth of C_{60} in both layers.

The same sample was then transferred to the preparation chamber and exposed to a partial pressure of 5×10^{-6} mbar chlorine gas for 45 min. Figure 1(b) shows an appropriate 1000×1000 nm^2 overview of the halogenated surface. Parts of the bare substrate covered with the bigger islands of the first monolayer and the fractal shaped clusters of the topmost layer are still discernible but a remarkable change in the island shapes can be observed. While the inner region of the C_{60} deposits have remained undistorted and still reveal (111) coordination [Fig. 2(a)] the structure of the island edges, especially in the first monolayer, is strongly affected. In an area up to 200 nm from the cluster edges only an inhomogeneous fullerene coverage can be found. Roundish holes that vary between 5 nm and 80 nm in diameter are statistically distributed in this region so that the VSe_2 substrate becomes visible. A close-up view of 60×60 nm^2 given in Fig. 2(b) illustrates this effect of disorder. Furthermore, single C_{60} molecules are not clearly identifiable although the STM should provide sufficient resolution. Therefore the STM data indicate a preferred chlorine aggregation at the C_{60} cluster edges, which leads to a perturbance of the fullerene coordination in the step regions. As the photoemission measurements in the following paragraph will provide further evidence for this interpretation, white boxes depict the appropriate zones in the schematic view in the upper corner of Fig. 1(b). With the help of STM only the morphology of the topmost fullerene layers can be monitored.

In order to gain insight into the chemical nature of the halogen-fullerene interaction the STM studies were combined with photoemission measurements. As a powerful tool to probe the electronic structure of the C_{60} sample the valence band and core level photoelectron spectra can be expected to show significant changes in the case of chemisorbed foreign particles that are covalently added to the C_{60} cage.[27,28]

In order to avoid a substrate influence in the measurements, a VSe_2 sample was covered with six monolayers of C_{60} and was then used to apply photoelectron spectroscopy. Figure 3 shows a comparison of the valence band spectra of

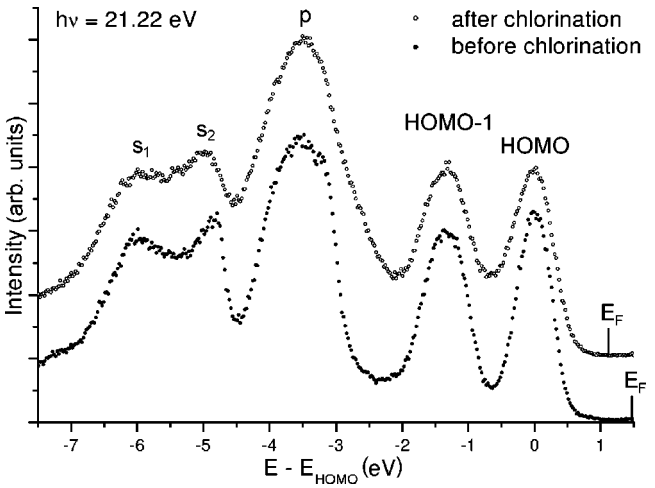

FIG. 3. The valence spectra of a six monolayer film C_{60} on VSe_2 before (bottom) and after chlorination (top) show all C_{60}-derived emissions are conserved (photon energy 21.22 eV).

the C_{60} surface before and after chlorination. The pristine sample (bottom) shows typical fullerene emissions that are well known from a number of previous publications. The energetic positions of the π-derived HOMO and HOMO-1 peaks at -1.48 eV and -2.84 eV (referred to the Fermi level E_F) agree well with the values of a former study[29] and indicate the absence of substrate-induced charge transfer or chemisorption effects, which are known from C_{60}-metal interfaces[30–32] with HOMO peak positions at about 2 eV below the Fermi level. The sample was subsequently exposed to a chlorine partial pressure of 6×10^{-6} mbar for 60 min and was then directly retransferred into the photoemission chamber where the second spectrum in Fig. 3 (top) was obtained. As the presence of foreign atoms may cause energetic shifts in photoelectron spectra,[31,33] both spectra were normalized to the HOMO peak energy in order to enable a direct comparison. In the chlorinated sample all C_{60} features are still clearly discernible. Careful evaluation of the π-derived peaks near E_F as well as the σ-derived emissions at higher binding energies reveals all relative peak positions unchanged while only a halogenation-induced broadening in the photoelectron peaks can be observed, which increases the averaged full width at half maximum (FWHM) values of about 30% and leads to generally higher count rates in the spectra minima. On the other hand, the count rates in the low-energy region of the spectra have remained nearly constant so that the amount of inelastically scattered electrons has not generally grown. Therefore the intensities in the peak maxima of both spectra may be directly compared. The fullerene-specific emissions HOMO-1 s_1 and s_2 are found with nearly constant count rates while only the HOMO peak undergoes an 11% decrease during chlorination. Furthermore, the remarkable feature p at about 4.5 eV below the Fermi energy shows an intensity increase of about 12%. The discussion of the chlorine core levels, which is presented later in the text, will show that changes in this energy region are likely to be attributed to Cl $3p$ emissions and will therefore not indicate the chemical affection of the fullerene cage.

As the spectrum of the chlorinated sample shows a strong

resemblance to UPS spectra of pure fullerene films a conservation of the valence band structure of the C_{60} crystal can be concluded even under exposure to chorine gas. Peak broadening and changes in the valence photoelectron intensities indicate the presence of adatoms, which was also predicted from the STM measurements, but a destruction of the molecular structure appears implausible so far. However, an evaluation of the Fermi level positions reveals an energetic shift of 370 meV in the C_{60} molecular orbital–related features towards lower binding energy following chlorination. Comparable shifts in both directions have been observed in a number of previous studies and are normally attributed to charge transfer effects. In fullerene-metal interfaces[33,31] the transfer of electronic charge from the metal conduction bands into the fullerene LUMO results in an enhanced screening of photogenerated holes. Therefore photoelectrons emitted from C_{60} molecules in an environment of metal atoms appear at lower binding energy in UPS and XPS spectra. On the other hand, in mixed compounds like the alkali-metal fullerides the alkali-metal *s* electrons that occupy the fullerene LUMO bands lead to an *n*-type doping of the entire C_{60} molecular crystal. Following a rigid-band model the Fermi level in photoemission measurements is thereby pinned near the LUMO position so that C_{60} valence emissions are located at higher binding energy in the spectra.

In the present chlorinated C_{60} sample a charge transfer into the fullerene LUMO bands is unlikely due to the strong electron affinity of the halogen. In contrast, a transfer of electronic charge from the fullerene molecules to surrounding chlorine particles may be possible. As the STM measurements of the preceeding paragraph indicate a mixed aggregation of C_{60} and chlorine in an area up to 200 nm from the cluster edges, a slight *p*-type doping of the fullerene crystal could be achieved. As this would mean the complementary process to the classical alkali-metal doping oppositely directed Fermi level pinning and shifts can be expected in photoelectron spectra. Further corroboration for this thesis will be given in the discussion of XPS measurements in one of the following paragraphs.

As the occupied electronic structure of the chlorinated fullerene sample has been found to be undistorted, x-ray absorption near-edge spectroscopy has been applied to gain information also about the unoccupied molecular orbitals. After chlorination XANES measurements were performed on the same sample that was used for the UPS measurements in the preceeding paragraph. Figure 4 compares a typical XANES spectrum of pristine C_{60} which was published by Luo *et al.*[34] with the absorption spectrum of our chlorinated C_{60} film. Although taken from different samples in different experimental environments the spectra show excellent agreement over a wide range of photon energies. The first four features between the absorption edge and the ionization threshold at 289.6 eV (Ref. 35) can be assigned to transitions from the C 1*s* core level to the LUMO bands.[36] Theoretical studies[35] as well as an experimental comparison between XANES data and inverse photoemission measurements[29] have proven the x-ray absorption spectroscopy to be dominated by a core hole-electron interaction so that the absorption spectra are not directly associated with the unoccupied

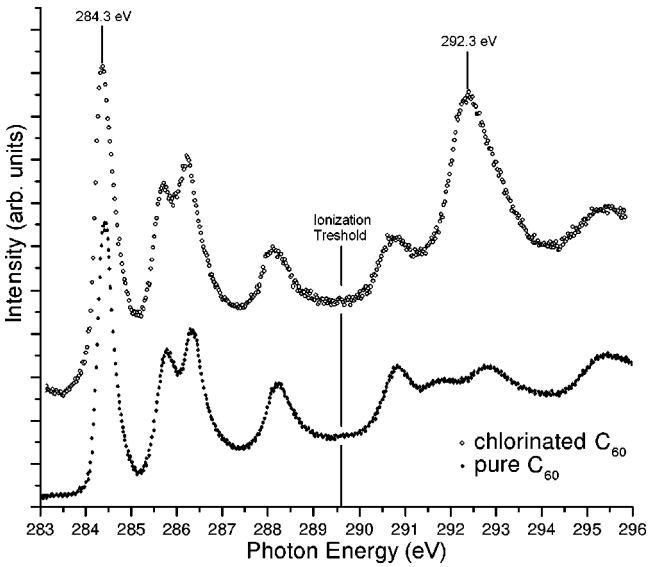

FIG. 4. The XANES spectra of pure C_{60} [bottom taken from Luo *et al.* (Ref. 34)] and of a chlorinated six monolayer film on VSe_2 (top) show identical LUMO-derived features and a chorine-induced peak at 292.3 eV.

density of states (UDOS). However, in the case of C_{60} the structures near the absorption edge are derived from LUMO states and may therefore be used to study how the unoccupied orbitals are affected. The fact that the profiles in the appropriate photon energy range are identical in both spectra indicates the conservation of the unoccupied electronic structure of C_{60} even during chlorination. The molecular structure of C_{60} can therefore be assumed to remain unchanged during the halogenation process. On the other hand, XANES peaks beyond the ionization threshold represent multiple scattering resonances and are interpreted as transitions into antibonding states. Thereby the chlorinated sample shows a significant structure at 292.3 eV, which seems to be added to the C_{60} absorption profile without any influence on the other emissions. Although the interpretation of this feature which may belong to chlorine-derived σ^* states, remains uncertain without any theoretical background, the presence of an additional resonance above the ionization threshold indicates an altered environment of scattering centers in the direct neighborhood of the carbon atoms. Consequently the profile of the XANES spectrum coincides with the interpretation of adsorbed chlorine particles next to the fullerene molecules without any covalent interaction.

After the investigations concerning the chemical structure of the chlorinated C_{60} sample the question arises if the interaction between halogen and fullerene is limited to the region close to the surface or if an interdiffusion process comparable to alkali-metal doping leads to an incorporation of halogen particles into the fullerite lattice. The STM measurements of the preceeding paragraph indicated chlorine aggregates in the step regions of the topmost fullerene islands but could not gain information on the underlying layers. Therefore, XPS studies have been performed under various detection angles. As shown in Fig. 5 the measurements taken with 339.35 eV photon energy on the chlorinated fullerene surface

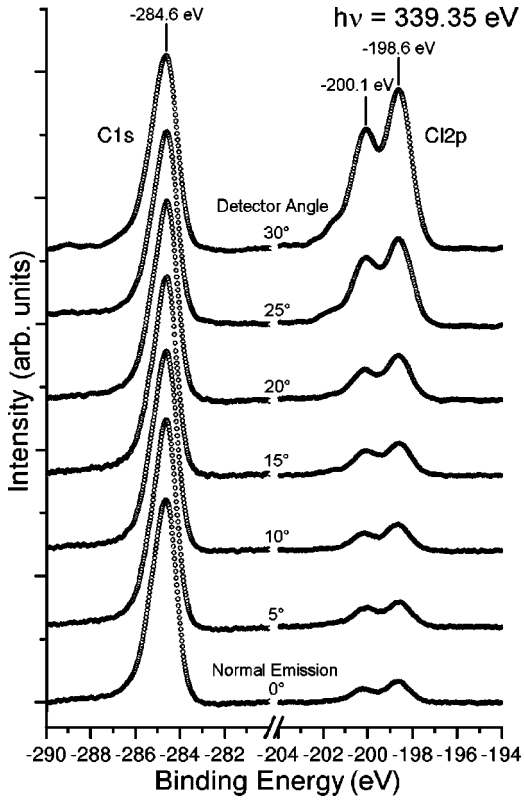

FIG. 5. The carbon and chlorine core level spectra indicate a preferred surface adsorption of chlorine particles with negligible chemical interaction with C_{60} (all spectra normalized to C 1*s* intensity).

reveal two dominant emissions that originate from carbon 1*s* and chlorine 2*p* core levels. No additional structures could be found at other kinetic energies, indicating a high-quality sample with only C_{60} and chlorine components. In all spectra the C 1*s* profile appears unchanged in width and line shape and is directly comparable to pure C_{60} samples. The binding energy derived from the main peak can be located at -284.6 eV. This value agrees with former publications where the C 1*s* position for bulk C_{60} was determined to lie between -285.2 eV and -284.9 eV for various metallic substrates. So the C 1*s* peak of the chlorinated sample still exhibits an energetic displacement of about 300 meV towards lower binding energies, which reproduces the shift observed in the valence band spectra. Therefore UPS and XPS prove a Fermi level movement, as can be expected after a charge transfer process from C_{60} to the halogen. The absence of electron donors such as metal atoms on the surface that could provide additional electronic charge for an enhanced screening of photogenerated holes marks the difference from previous publications dealing with shifted photoemission spectra towards lower binding energy from fullerene-metal structures.[30,31,33] On the other hand, the present results agree well with the work of Ohno *et al.*,[21] who evaporated iodine gas onto fullerene samples and reported C 1*s* core level shifts towards lower binding energy of about 200 meV for a noncovalent sample stoichiometry of $C_{60}I_{0.04}$. Although the amount of charge transfer was estimated to be very small Ohno *et al.* assumed iodine atoms to serve as electron acceptors for C_{60}.

As shown in the right-hand side of Fig. 5 the halogen in our chlorinated sample is clearly identifiable. Under all emission angles a peak doublet from Cl $2p_{1/2}$ and Cl $2p_{3/2}$ core level emissions can be found at -200.1 eV and -198.6 eV binding energy, respectively. These values reproduce well the findings of former XPS measurements[37] on chlorine-containing salts where the averaged Cl 2*p* binding energy was given as -199 eV and prove the presence of adsorbed chlorine particles on the fullerene sample. As the Cl $2p_{3/2}$ binding energy for covalently bonded carbon-chlorine compounds like polyvinyl chloride or chlorobenzene was reported to lie at about -200 eV,[37] another indication for a noncovalent interaction can be derived.

So the fullerene as well as the halogen core level emissions corresponds to the results of the STM UPS and XANES studies. Furthermore, the Cl 2*p* binding energy can be used to estimate the position of the chlorine 3*p* emissions referred to the Fermi level E_F. As Yeh and Lindau,[38] who calculated element-specific binding energies for free atoms referred to the vacuum level, found a difference of 195.5 eV between the averaged Cl 2*p* and Cl 3*p* levels the Cl 3*p* peaks can be estimated to lie at approximately -3.5 eV binding energy in the present measurements. Increased count rates or asymmetric C_{60} profiles near -4 eV binding energy in the valence spectra may therefore be related to Cl 3*p* emissions that overlay the fullerene-derived profile although the number of emitted Cl 3*p* photoelectrons can be expected to be very small due their weak ionization cross section compared with carbon valence electrons.[38]

As a basic principle XPS spectra obtained in normal emission mode are not sufficient to identify possible adsorbates or intercalates. In order to monitor a *z*-dependent chlorine concentration gradient the following XPS measurements were performed under variable detection angles. As illustrated at the bottom of Fig. 5 the normal emission measurements are dominated by carbon photoelectrons with a C 1*s*/Cl $2p_{3/2}$ intensity ratio of 9.74 (derived from the maximum count rates). Based on the photon energy of $h\nu = 339.35$ eV the kinetic energy of excited carbon and chlorine core level electrons may easily be derived. In accordance with former measurements[39] that focused on comparable photoelectrons emitted from a fullerene film, their mean escape depth can therefore be estimated to exceed 5 Å. Referred to the molecular centers of the topmost layer, this value is sufficient to reach the topmost octahedral fullerite lattice sites at 4.09 Å as well as the tetrahedral sites at 2.73 Å. While the sample's orientation to the synchrotron light source was kept unchanged, the analyzer angle was then increased from normal emission in order to decrease the photoemission information depth. Consequently the experiment became more surface-sensitive. As larger angles lead to generally decreased count rates, on the other hand, all spectra had to be normalized to the C 1*s* intensity to gain information about the fullerene-halogen photoelectron ratio at various escape depths. Figure 5 depicts the normalized carbon and chlorine XPS spectra at different detection angles between 0° (normal emission) and 30°. With increasing angle a remarkable enhancement of the

relative Cl $2p$ intensities can be observed. Compared to normal emission conditions the Cl $2p$ intensity has grown by factor 8.27 at 30° so that the C $1s$/Cl $2p_{3/2}$ intensity ratio is reduced to 1.18. As the mean electron information depth at this angle is only decreased to approximately 4.3 Å, a very strong angular dependency in the intensities can be stated, indicating a preferred surface adsorption of chlorine particles on the fullerite film. In accordance with the STM data we conclude that the halogen deposition is energetically favored at steplike sites next to the fullerene island edges. As proven by the STM data thereby small amounts of weakly bonded C_{60} molecules may be released from their former (111)-coordinated positions leading to an inhomogeneous but mixed fullerene-chlorine coverage in the appropriate regions. Regardless of the oxidization potential of chlorine gas the C_{60} molecular cage remains structurally unchanged during the aggregation process although a charge transfer process to the halogen may be derived from the shifted XPS and UPS spectra. However, based on the evaluation of the XPS data an interdiffusion process of the halogen cannot generally be excluded. The present data merely confirm the major amount of chlorine to be deposited on the fullerite surface.

Furthermore, especially at 30° a small shoulderlike structure becomes visible in the Cl $2p$ profile at approximately -201.5 eV binding energy. As this feature cannot be observed at smaller emission angles it seems to be attributed to chlorine particles on the sample surface. While the absence of a chemically shifted component in the C $1s$ spectra does not allow the association with a carbon-chlorine covalent bonding the appropriate photoelectrons may originate from chlorine atoms that have not intermixed with fullerene molecules on top of the sample surface. Therefore two chemical environments are possible for adsorbates on the topmost fullerene layer. The major part of chlorine particles will form a mixed halogen-fullerene coverage accompanied by a charge transfer process. On the other hand, due to incomplete interdiffusion a small amount of chlorine may remain in the direct neighborhood of other halogen atoms. Consequently no charge transfer processes will take place, leading to small Cl $2p$ components at higher binding energy in the surface-sensitive XPS spectra.

The results of the preceeding paragraph have shown that an exposure of C_{60} films to chlorine gas under vacuum conditions will not lead to a homogeneous distribution of halogen particles in the fullerite lattice as could be expected after a complete intercalation. Instead the major amount of the halogen remains on the sample surface. In view of possible analogies to alkali metals the question arises if an increased chlorine incorporation can be achieved artificially by use of a different preparation method. As shown in a number of previous works[16–19] for C_{60} and iodine, a combination of fullerene and halogen under bulk conditions is possible. For evaluation of this question an alternating preparation sequence of fullerene and chlorine deposition was applied. First a 0.64 monolayer film of C_{60} was evaporated onto a VSe_2 substrate. In analogy to the STM studies that were presented earlier the sample was then exposed to a chlorine gas pressure of 5×10^{-6} mbar for 45 min. In the next step the same sample was used for deposition of another 0.64 monolayer C_{60} in order to perform further STM measurements. Figure 6 shows the geometric structure of the surface in an area of 2000×2000 nm^2. The island shapes of the first and the second monolayer can easily be recognized because of their chlorinated edges, which stick out in light colors. Compared with Fig. 1(b) the edge regions now appear brighter due to new fullerene material that has grown on top of the chlorinated zones. In fact the chlorinated area seems to act as a preferential growth site as a careful inspection also reveals new C_{60} deposits aggregated next to the chlorinated zones, which could not be observed in the surface morphology of Fig. 1(b). On one hand, the islands of both layers are now decorated with new fullerene material up to 150 nm width that has grown away from the cluster centers increasing the average island diameter. On the other hand, new clusters in the second layer (up to 100 nm width) have grown towards the island centers outgoing from the chlorinated edges of the first monolayer. Some of the new deposits in the first and the second fullerene layer have been highlighted with arrows in Fig. 6. Therefore the halogenated island edges may be classified as growth seeds for subsequent fullerene deposition so that a second C_{60} evaporation will obviously lead to enclosed amounts of chlorine. This fact is schematically illustrated in the sideview in the top right corner of Fig. 6.

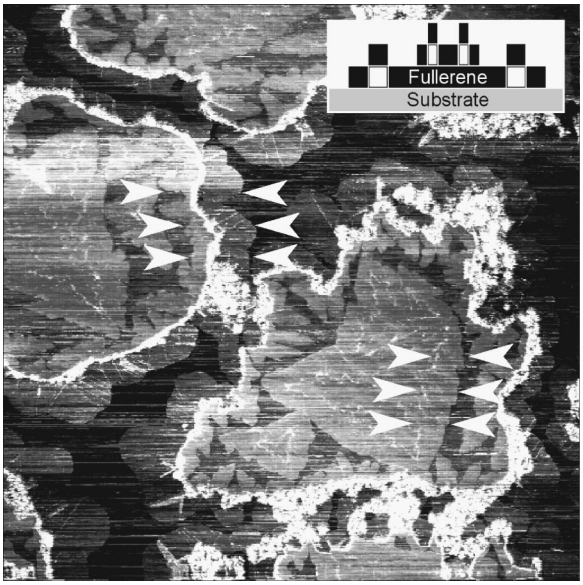

FIG. 6. STM images of chlorinated 0.64 monolayer C_{60} on VSe_2 after subsequent fullerene deposition show new material besides and on top of the chlorinated island edges (marked with arrows) (dimension, 2000×2000 nm^2; bias, $+1.52$ V, $I_T=0.57$ nA).

In order to monitor the C_{60} aggregation on top of the chlorinated island edges topographic profiles were used. The bottom part of Fig. 7 depicts a height-sensitive scan over 1000 nm along the white line in the upper STM picture, which was taken from Fig. 6. With the help of the emphasized island edges, which originate from the chorination process, the island dimensions in both C_{60} layers before the second fullerene evaporation are still discernible. Therefore the new fullerene material of the second deposition is clearly

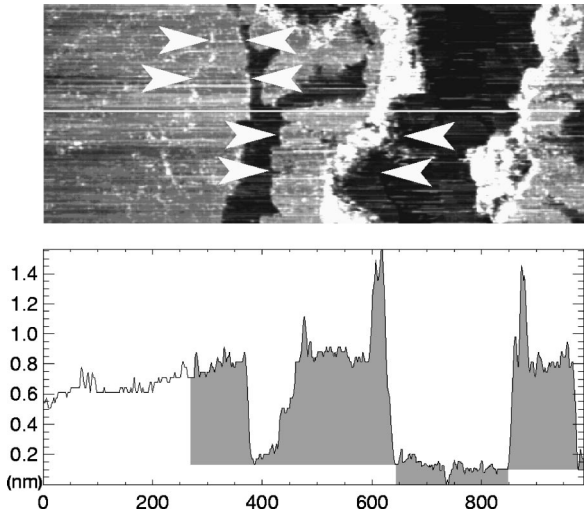

FIG. 7. Topographic profile of a chlorinated C_{60}/VSe_2 surface after subsequent fullerene deposition [new material: marked with arrows (top) colored gray (bottom)]. Chlorinated island edges act as growth seeds (bias, +1.5 V; $I_T = 0.57$ nA).

identifiable and has been marked with arrows. In the profile graph the new deposits have been highlighted with gray color, whereby the major part is located next to the chlorinated zones in both layers. However, additional aggregations directly on top of the halogenated areas are visible, which appear as peaklike features. This kind of growth, which cannot be observed on pristine C_{60} samples confirms the chlorinated island edges to serve as seed regions not only for two-dimensional but also for three-dimensional fullerene growth. Therefore a sample preparation with alternating fullerene and chlorine depositions appears suitable for growing more complicated multilayer structures with small amounts of incorporated chlorine. Although this procedure will probably not lead to the formation of well-ordered chlorine sublattices or fullerene-halogen compounds with defined stoichiometry, the technique offers the possibility to combine both materials without covalent interaction and to achieve conditions that strongly resemble C_{60}–alkali-metal interaction.

IV. CONCLUSIONS

In the present paper epitaxial fullerene films had been exposed to chlorine gas under vacuum conditions and at room temperature. The sample surfaces were studied with scanning tunneling microscopy (STM) ultraviolet and x-ray photoemission spectroscopy (UPS and XPS) and x-ray absorption near-edge spectroscopy (XANES). A combination of the different methods on one sample revealed the following major findings. (i) Chlorine deposits can be observed in an area up to 200 nm from the C_{60} island edges where the former (111) coordination is disturbed and has been replaced by an inhomogeneous coverage of fullerene and chlorine particles. Additional XPS studies confirmed the major amount of chlorine to be aggregated on the fullerene film surface although a partial interdiffusion of the halogen cannot be excluded. (ii) As proven by UPS and XANES measurements the C_{60} cage structure is not affected by the adsorption process. However, a Fermi level movement and the Cl $2p$ emissions comparable to ionic salts indicate a charge transfer process from C_{60} to the halogen. (iii) The chlorinated regions on the topmost layers serve as growth seeds for subsequent C_{60} deposition. New fullerene material will aggregate next and on top of the chlorinated regions so that an alternating C_{60}-chlorine deposition sequence will lead to an incorporation of small halogen amounts.

Outgoing from these conditions future measurements will show if further analogies to or differences from alkali-metal fullerides or from iodinated C_{60} films can be derived for chlorinated fullerene samples. In particular, resistivity measurements and annealing experiments will be of interest as generation of charge carriers and the diffusion of adsorbed halogen particles still have to be examined. But also combination of halogenation and *n*-type doping appears interesting in view of a possible I-VII compound formation.

ACKNOWLEDGMENTS

We acknowledge experimental support by K. Roßnagel. This work was supported by the BMBF (Project 05 SE8 FKA and 05 SB8 FKB).

*Author to whom correspondence should be addressed.

[1] H. Kroto, J. R. Heath, S. C. O'Brian, R. F. Curl, and R. E. Smalley, Nature (London) **318**, 162 (1985).
[2] W. Krätschmer, L. Lamb, K. Fostiropoulos, and D. Huffmann, Nature (London) **347**, 355 (1990).
[3] A. Hebard, M. J. Rosseinsky, R. C. Haddon, D. W. Murphy, S. H. Glarum, T. T. M. Palstra, A. P. Ramirez, and A. R. Kortan, Nature (London) **350**, 600 (1991).
[4] K. Holczer, O. Klein, S. M. Huang, R. B. Kanera, K. J. Fu, R. L. Whetten, and F. Diederich, Science **255**, 1154 (1991).
[5] M. Rosseinky, A. P. Ramirez, S. H. Glarum, D. W. Murphy, R. C. Haddon, A. F. Hebard, T. T. M. Palstra, A. R. Kortan, S. M. Zahurak, and A. V. Makhija, Phys. Rev. Lett. **66**, 2830 (1991).
[6] T. T. M. Palstra, Solid State Commun. **93**, 327 (1995).
[7] N. Laouini, O. Andersen, and O. Gunnarsson, Phys. Rev. B **51**, 17 446 (1995).
[8] M. DeSeta and F. Evangelisti, Phys. Rev. B **51**, 6852 (1995).
[9] G. Zhang, R. T. Fu, X. Sun, K. H. Lee, and T. Y. Park, Phys. Lett. A **199**, 391 (1995).
[10] M. Dresselhaus G. Dresselhaus, and P. Eklund, *Science of Fullerenes and Carbon Nanotubes* (Academic Press, San Diego, 1996).
[11] P. Birkett, P. B. Hitchcock, H. W. Kroto, R. Taylor, and D. R. M. Walton, Nature (London) **357**, 479 (1992).
[12] F. Tebbe, R. L. Harlow, D. B. Chase, D. L. Thorn, G. C. Campbell, Jr., J. C. Calabrese, H. Herron, R. J. Young, Jr., and E. Wasserman, Science **256**, 822 (1992).
[13] G. Olah, I. Bucsi, C. Lambert, R. Aniszfeld, J. Trivedi, D. K. Sunsharmo, and G. K. Surya Prakash, J. Am. Chem. Soc. **113**, 9385 (1991).
[14] A. Tuinman, P. Mukherjee, J. L. Adcock, R. L. Hettich, and R. N. Compton, J. Phys. Chem. **96**, 758 (1992).
[15] J. Holloway, E. G. Hope, R. Taylor, G. L. Langley, A. G. Avent, T. J. Dennis, J. P. Hare, H. W. Kroto, and D. R. M. Walton, J.

Chem. Soc. Chem. Commun. **9**, 966 (1991).
[16] M. Limonov, Y. E. Kitaev, A. V. Chugreev, V. P. Smirnov, Y. S. Grushko, S. G. Kolesnik, and S. N. Kolesnik, Phys. Rev. B **57**, 7586 (1998).
[17] S. Nakashima, M. Norimoto, H. Harima, Y. Hamanaka, L. S. Grigoryan, and M. Tokumoto, Chem. Phys. Lett. **268**, 359 (1997).
[18] Q. Zhu, D. E. Cox, J. E. Fischer, K. Kniaz, A. R. McGhie, and O. Zhou, Nature (London) **355**, 712 (1992).
[19] Y. Grushko, G. Wortmann, M. F. Kovalev, L. I. Molkanov, Y. V. Ganzha, Y. A. Ossipyan, and O. V. Zharikov, Solid State Commun. **84**, 505 (1992).
[20] H. Werner, M. Wesemann, and R. Schlöge, Europhys. Lett. **20**, 107 (1992).
[21] T. R. Ohno, G. H. Kroll, J. H. Weaver, L. P. F. Chibante, and R. E. Smalley, Nature (London) **355**, 401 (1992).
[22] Y. Miyamoto, A. Oshiyama, and S. Saito, Solid State Commun. **82**, 437 (1992).
[23] R. Schwedhelm, J.-P. Schlomka, S. Woedtke, R. Adelung, L. Kipp, and M. Skibowski, Phys. Rev. B **59**, 13 394 (1999).
[24] The fullerene powder was obtained from Hoechst AG (Germany), C_{60} purity 99.78%, C_{70} content 0.2 ppm (1998).
[25] The chlorine gas was obtained from Messer Griesheim GmbH (Germany), purity 99.98% (1997).
[26] Standard Micro-STM from Omicron (Germany) (1993).
[27] P. J. Benning, T. R. Ohno, B. I. Dunlop, J. H. Weaver, P. Mukherjee, J. L. Adcock, and R. N. Compton, Phys. Rev. B **47**, 1589 (1993).
[28] F. H. Jones, M. J. Butcher, B. N. Cotier, P. Moriarty, P. H. Beton, V. R. Dhanak, and F. Wudl, Phys. Rev. B **59**, 9834 (1999).
[29] R. Schwedhelm, L. Kipp, A. Dallmeyer, and M. Skibowski, Phys. Rev. B **58**, 13 176 (1998).
[30] A. J. Maxwell, P. A. Brühwiler, A. Nilsson, N. Mårtenson, and P. Rudolf, Phys. Rev. B **49**, 10 717 (1994).
[31] G. Wertheim and D. Buchanan, Phys. Rev. B **50**, 11 070 (1994).
[32] N. Swami, H. He, and B. Koel, Phys. Rev. B **59**, 8283 (1999).
[33] D. Owens, C. Aldao, D. Poirier, and J. Weaver, Phys. Rev. B **51**, 17 068 (1995).
[34] Y. Luo, H. Ågren, and F. Gel'mukhanov, Phys. Rev. B **52**, 14 479 (1995).
[35] M. Nyberg, Y. Luo, L. Triguero, L. G. M. Pettersson, and H. Ågren, Phys. Rev. B **60**, 7956 (1999).
[36] J. Stoehr, *NEXAFS Spectroscopy*, Vol. 25 of *Springer Series in Surface Science* (Springer, Berlin, 1996).
[37] C. Wagner, W. Riggs, L. Davis, and J. Moulder, in *Handbook of X-Ray Photoelectron Spectroscopy*, edited by G. Muilenberg (Perkin Elmer, Eden Prairie, Minnesota, 1979).
[38] J. Yeh and I. Lindau, in *Atomic Subshell Photoionization Cross Sections and Asymmetry Parameters: $1 \leqslant Z \leqslant 103$*, Vol. 32 of *Atomic Data and Nuclear Data Tables*, edited by A. Li-Scholz (Academic Press, New York, 1985).
[39] G. Wertheim, D. Buchanan, E. Chaban, and J. Rowe, Solid State Commun. **83**, 785 (1992).